

Mechanism and kinetic modelling of PEEK pyrolysis by TG/MS

L.H. Perng^{a,*}, C.J. Tsai^b, Y.C. Ling^c

^aDepartment of Chemical Engineering, Ta Hwa Institute of Technology, Chung-lin, Hsinchu 30703, Taiwan

^bCenter for Aviation and Space Technology, Industrial Technology Research Institute, Hsinchu 310, Taiwan

^cDepartment of Chemistry, National Tsing Hua University, Hsinchu 30043, Taiwan

Received 8 September 1998; received in revised form 26 October 1998; accepted 21 December 1998

Abstract

A new technique combining Py-GC/MS with TG/MS can be used in analyzing the mechanism and kinetic modelling of pyrolysis. The results of this study show that a combined approach of Py-GC/MS and TG/MS exhibited dynamic curves of 13 evolved gases from the pyrolysis of PEEK from room temperature to 900°C. In this study we also discovered that there are two stable pyrolysis reaction regions during the pyrolysis in helium atmosphere at a heating rate of 10°C/min from room temperature to 900°C. In the first pyrolysis region the ether group and ketone group from the main chain of PEEK decomposed to phenol and CO₂, respectively. It also showed that the thermal stability of the ketone group was better than that of the ether group. Accompanied with the chain transfer in the first pyrolysis region, the fluorenone structure appeared in part of the carbonization scheme. Above 650°C it moved to the second reaction region. In this region the main decomposition products were CO₂ from the ketone group of fluorenone and from the carbonized structure described above. From the two flat regions of the activation energy curve of pyrolysis, we have proposed a kinetic model with two pyrolysis regions. Based on this model, we compared the theoretical pyrolysis curve with the experimental curve, the two curves being quite similar. © 1999 Elsevier Science Ltd. All rights reserved.

Keywords: PEEK pyrolysis; Mechanism and kinetic model; Py-GC/MS and TG/MS

1. Introduction

The analysis of the pyrolysis of polymers is very crucial to designing, processing temperature and application of polymers. Recent systematic investigations about the pyrolysis characteristics and mechanisms have helped us to improve their backbone structures, achieving higher thermal durability.

PEEK is a half-crystalline plastic with high thermal durability used in engineering. It also resists organic solvents, chemical corrosion, ignition, and can be easily adapted for processing. This is the reason why it has been evaluated recently for the possibility to replace conventional thermally durable materials and spare parts used by aircraft and automobiles. It means that more research and evaluation will be required, among which its pyrolysis behavior and mechanism is of paramount importance.

There have been numerous ways to evaluate the pyrolysis behavior of PEEK in the literature, however, most of them were limited to the kinetics and mechanisms around the temperature region of initial pyrolysis. Day [1–3] obtained

the parameters of the isothermal pyrolysis of TGA at temperatures between 390°C and 528°C and constant heating rate between 460°C and 520°C; similarly Kenny [4] studied the thermogravimetric loss of PEEK/carbon fiber composites between 450°C and 515°C. Salin [5] used high resolution TGA to analyze the kinetic parameters. Hay [6] evaluated the pyrolysis mechanism by Py-FT/IR and the identification of reaction products comprising phenol, benzofuran and oligomers with –OH group. Cole [7] used FTIR to observe the thermal pyrolysis of PEEK and PEK-carbon composite in air and nitrogen between 400°C and 485°C. Day [8] investigated the PEEK pyrolysis with Py-GC/MS and used GC/MS to identify the distribution of 14 pyrolyzed products under different temperatures to propose possible mechanisms in pyrolysis. However, the traditional once-through flash pyrolysis such as Py-GC/MS under various temperatures for pyrolysis of polymers is unable to differentiate the major reaction mechanisms and product distribution at specific temperature regions; as a consequence this area for investigation remains unexplored.

The use of weight loss in TG analysis is not as versatile in mechanism evaluation as by the direct analysis of evolved gas mixture and associated solid residue; nevertheless, the latter is most likely under the interference of crosslinking of

* Corresponding author. Tel.: + 886-3-5923551; fax: + 886-3-5927310.
E-mail address: cep1h@et4.thctc.edu.tw (L.H. Perng)

Table 1
Selective non-disturbance ion species in TG/MS analysis of PEEK pyrolysis

Peak number	Compound	Ion species (<i>m/e</i>)
1	Carbon dioxide	44
2	Water	18
3	Benzene	78
4	<i>p</i> -Benzoquinone	108
5	Phenol	94
6	Naphthalene	128
7	Hydroquinone	110
8	Biphenyl	154
9	Diphenylether + phenylphenol	170
10	Dibenzofuran	168
11	Fluorene	166
12	Benzophenone	182
13	Dibenzofuranol	184

functional group in the polymer structure and not ideal for interpretation. Thus, the direct analysis of gas compositions by continuous monitoring with on-line TG/MS technique has gained more attention in the identification of gaseous components in the pyrolysis of polymers, in particular for mechanism studies. Recently, the development of TG/MS interface design has made significant breakthrough in stability. Such a system has been successfully used in studying the mechanisms of PEEK [8] and LCP [9] polymers, fire-retardant additive in PS [10] and various gaseous molecules [11]. Thus, the interface system has not reached the stage of perfection [12], and TG/MS has been used mostly in the analysis of small-size molecules, such as CO, CO₂, water and phenol. Our research team has successfully developed a novel interface system [13], which has high sensitivity and eliminates tailing phenomenon of total ion current (TIC) with real-time plotting of gas evolution curves in thermal pyrolysis of polymers.

It has to be pointed out that the TG/MS technique requires suitable operating conditions to enable the evolved gas mixture from TGA as the input stream to MS for analysis and identification. Thus, in this study we used the good resolution power of Py-GC/MS to analyze the specific, non-interfered ion species for *m/e* values in mass spectra, TG/MS to obtain the gas evolution curves and TG curves to obtain kinetic parameters, leading to the postulation of reaction mechanisms and the kinetic modelling of PEEK pyrolysis.

2. Experimental

2.1. Materials

The PEEK samples (trade name Victrex®) used in this study were obtained from ICI Petrochemical and Polymer Ltd. as commercial grade films (~0.085 mm in thickness).

2.2. Apparatus and procedures

2.2.1. Py-GC/MS [14]

The Py-GC/MS experiments were carried out using a CDS 2000 Pyroprobe pyrolyzer (Chemical Data System Co. Ltd.) coupled to an HP 5890 gas chromatograph fitted with an HP 5972 quadrupole mass spectrometer. The probe was calibrated by the manufacturer to ensure the accuracy of the nominally set temperatures. Sample aliquots (~1.00 mg) were pyrolyzed in a quartz sample holder capillary using the platinum coil attachment (5/16 in. diameter), and the temperature setting of the Pyroprobe was 900°C. The pyrolysis was carried out using helium carrier gas at a flow rate of 50 ml/min. The GC column was an HP-5MS (30 m by 0.25 mm i.d., 0.25 μm film thickness). Oven temperature was initially held for 2 min at 40°C, then programmed to 250°C at 10°C/min and held for 5 min; then programmed to 260°C at 10°C/min and held for 10 min. The GC/MS interface was set at 280°C. The flow rate was kept constant and E.I. was kept at 70 eV. The MSD was scanned from 10 to 400 *m/e* at a scan rate of 1.8 scan/s. Data analysis was carried out using an HP Chem Station G1034C (version 3.00) to match with NIST spectra by comparison.

2.2.2. TG/MS

The TG/MS experiments were carried out with a home designed high efficiency TG/MS system [13] by coupling TGA (DuPont TA 2950), modified CDS 3500 interface and HP 5972 quadrupole mass spectrometer. The sample was pyrolyzed by TGA and the evolved gas products entered the CDS 3500 interface through a deactivated column (0.53 mm i.d.) first, and then passed to the HP 5972 quadrupole mass spectrometer from a deactivated column (0.1 mm i.d.) of interface splitter for measuring the pyrolysates generation curve. The operating conditions were as follows: purge gas, helium of 99.9995% purity; temperature setting of interface, 300°C; MS range, 10–550 a.m.u.; scan rate, 1.2 scans/s; and two computer systems were used for controlling TGA and MS respectively.

3. Results and discussion

3.1. Mechanism studies of PEEK pyrolysis using TG/MS and Py-GC/MS

In order to identify a complicated mixture of ion species from TG/MS, this study attempted to combine the superior separating and identifying ability of Py-GC/MS to analyze pyrolysates of PEEK. Then, the results was used to select non-disturbance specific ion species (*m/e*) for TG/MS to investigate the real-time generation curve of pyrolysates.

The typical chromatogram and mass spectra of the pyrolysates obtained by flash pyrolysis of PEEK at temperatures up to 900°C in helium atmosphere were shown already in Ref. [14]. The 21 major pyrolysates were identified by their mass spectra. Selective spectra were determined by

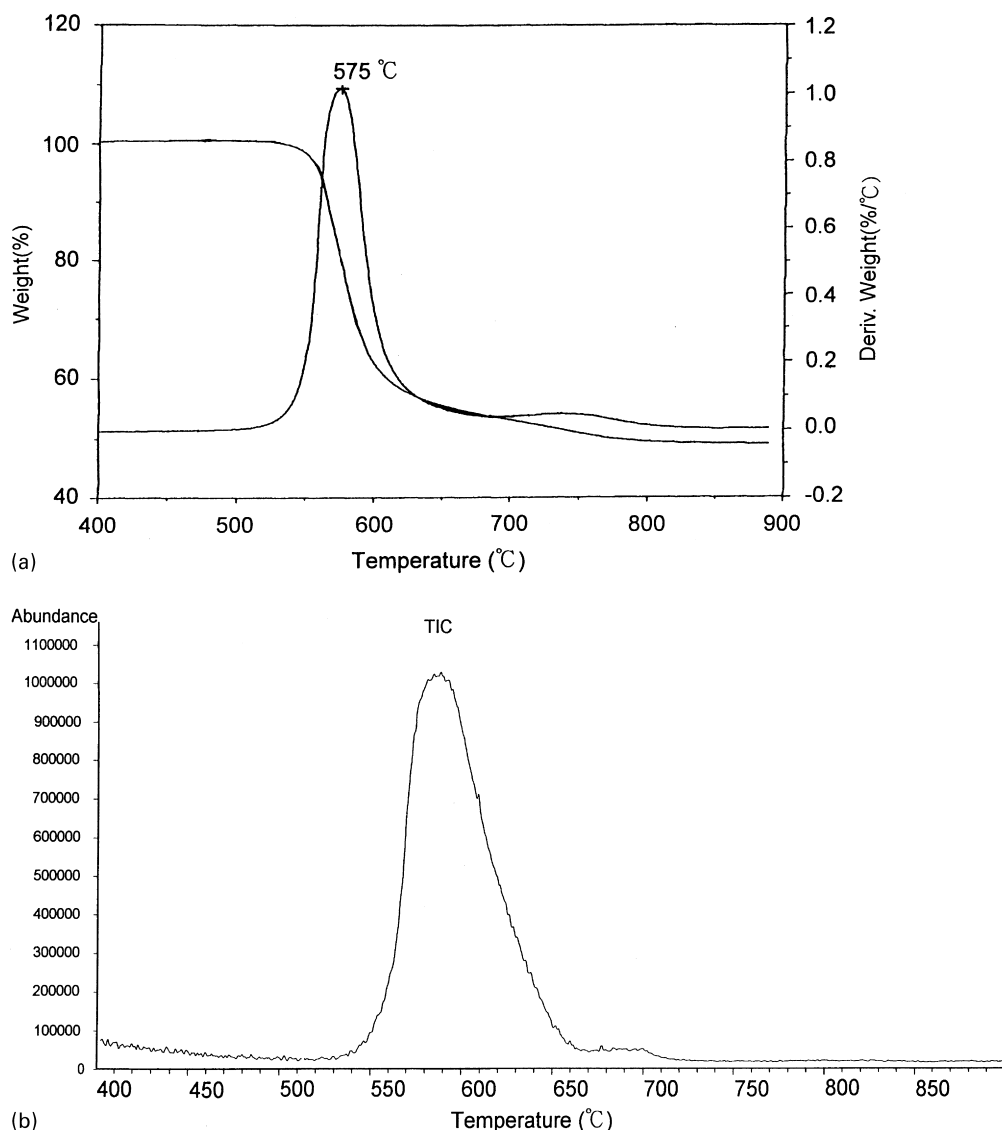


Fig. 1. TG/MS analysis of PEEK pyrolysis in He at 10°C/min: (a) TG/DTG curve; and (b) TIC in mass spectrum.

comparing the mass spectra of the pyrolysates for TG/MS analysis, in which appropriate selective non-disturbance ion species (m/e) can be chosen for analyzing all the pyrolysates except for two groups of pyrolysates, they are No. 9 (diphenyl ether) and No. 13 (phenyl phenol); and No. 20 (4-phenoxy-1-1-[4-hydrobenzophenone]) and No. 21 (1-phenoxy-4-[4-phenoxy-1-aldehyde]), which cannot be segregated because of the same m/e values. From the TG/MS spectra, the results of the small molecular species using specific non-disturbance ion species of individual pyrolysates are listed in Table 1; and 13 pyrolysates are identified by the TG/MS system in this study. Besides, the contamination of air in the TG furnace will oxidize the pyrolysates of CO from ketone group and hydrogen radical into CO₂ and H₂O, respectively. The evolution profiles of PEEK from TG, DTG, and TIC in helium atmosphere at a heating rate of 10°C/min from room temperature to 900°C analyzed by TG/MS are shown in Fig. 1(a) and (b). According to the results

shown in Fig. 1(a) and (b), two pyrolysis reaction regions can be identified. The DTG pyrogram shows that the maximum pyrolysis reaction rate occurred at 575°C in the first pyrolysis reaction and the second pyrolysis reaction at above 650°C. Similar to the DTG pyrogram, the TIC pyrogram also shows two pyrolysis reaction regions. Four major pyrolysate generation curves of PEEK (phenol, CO₂, dibenzofuran, and benzene) using TG/MS were obtained at temperatures up to 900°C in helium atmosphere as shown in Fig. 2(a), which shows a peak maximum of phenol at the lowest temperature; then CO₂, benzene, and dibenzofuran with the order of increasing temperatures. In addition, two peak maxima were noticed in the CO₂ pyrogram; and the temperature of peak maximum in the second pyrolysis reaction was the same by comparing the CO₂ pyrogram in Fig. 2(a) and the TIC pyrogram in Fig. 1. Therefore, we may predict that the main chain random scission of the ether and ketone groups of PEEK in the first reaction is the major

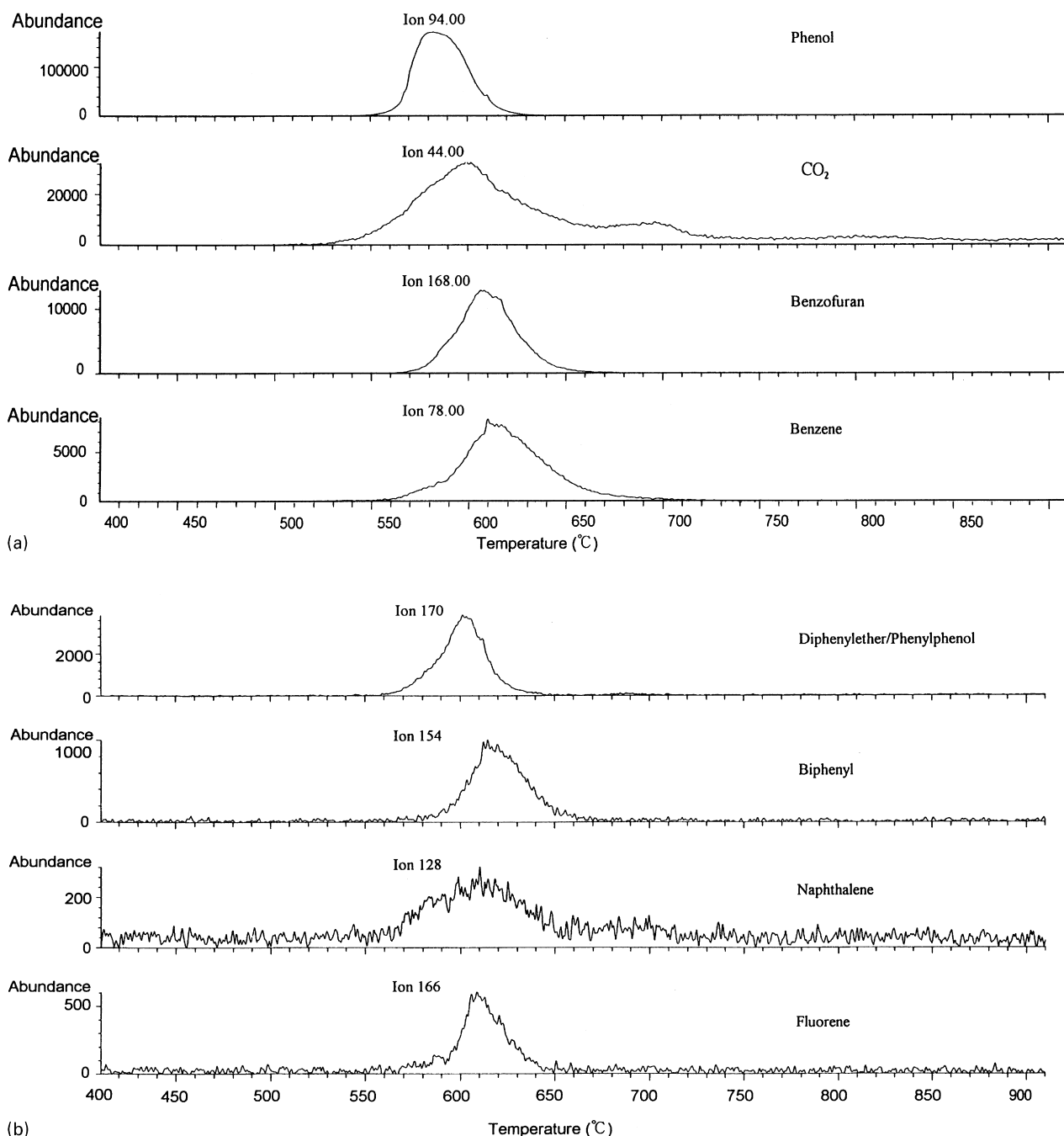


Fig. 2. TG/MS curves of product from PEEK pyrolysis in He at 10°C/min: (a) phenol, CO₂, benzofuran and benzene; (b) diphenylether/phenylphenol, biphenyl, naphthalene and fluorene; and (c) *p*-benzoquinone, hydroquinone and water.

pyrolysis mechanism, and the ether group scission reaches a maximum value earlier than that of the ketone group. Further, the pyrolysates in the second reaction may be formed from the decomposition of the new structure with higher thermal stability, and this will be discussed later and confirmed by analysis of the solid residue.

The generation curves of pyrolysates, such as diphenylether (or phenyl phenol), diphenyl, naphthalene, and fluorene, as a function of peak pyrolysis temperature are shown in Fig. 2(b). These pyrolysates were formed by the

recombination of free radicals which were products of main chain scission. Diphenyl, naphthalene, and fluorene were produced at the temperature of peak maximum at about 615°C; while diphenylether (or phenyl phenol) was produced at about 600°C. The peak maximum formed in the latter portion of the first pyrolysis reaction indicates that these pyrolysates have more opportunity to form due to the scission of ketone group. Additionally, the results showed that the chain transfer in the carbonization mechanism takes place in the first pyrolysis reaction.

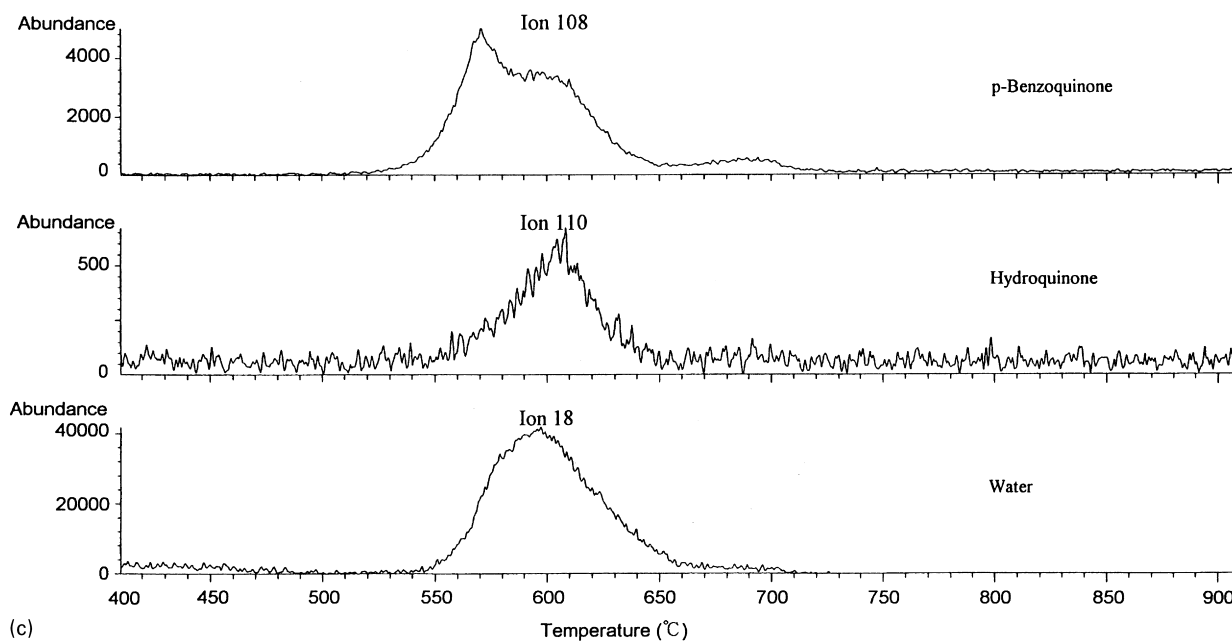


Fig. 2. (continued)

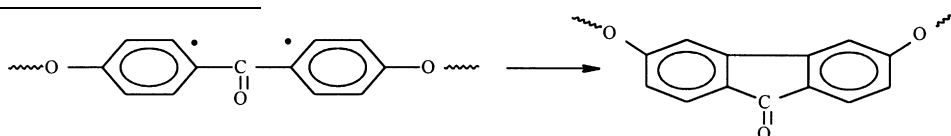
Table 2
Elemental analysis of solid residue from PEEK pyrolysis

Sample	Result		
	%C	%H	%O
PEEK (theo.)	79.2	4.1	16.7
Film not heated	79.5	4.5	16.1
Solid residue (650°C)	83.3	3.7	13.0
Solid residue (800°C)	88.7	3.3	8.0
Solid residue (900°C)	90.2	3.1	6.6

Pyrolysate generation curves of *p*-benzoquinone, hydroquinone, and water are shown in Fig. 2(c). Observing the pyrogram of *p*-benzoquinone, three peak maxima were formed at 575°C, 590°C, and 695°C respectively, two peak maxima (575°C and 590°C) occurred in first pyrolysis reaction region and the third (695°C) in the second pyrolysis reaction region. Nevertheless, hydroquinone and water were formed with only one peak maximum at 590°C. This observation indicated that *p*-benzoquinone was formed by decomposition of ether group, and hydroquinone could not be formed because of the mass production of phenol inhibiting the reaction of *p*-benzoquinone with hydrogen radical to form hydroquinone. But when the ketone group became the dominating mechanism at the latter stage of first pyrolysis reaction, mass production of *p*-benzoquinone occurred again and had good opportunity to react with the hydrogen

radical to form hydroquinone with only a small amount of phenol remaining. Thus, hydroquinone formed predominantly at 590°C. The peak maximum of *p*-benzoquinone at 695°C was accompanied by the decomposition of the new stable structure in the second pyrolysis reaction region. And in this period hydroquinone could not be formed due to lack of hydrogen radical, which can be confirmed from the absence of water in the second pyrolysis reaction.

In order to confirm the formation of the fluorenone type structure and the prediction as described earlier, the pyrolysis temperature of the PEEK sample was increased to 650°C, 800°C, and 900°C, in helium atmosphere using TGA. Then the solid residue and the pure PEEK (film without pyrolysis) were analyzed through comparison of the elements. The result of elemental analysis in Table 2 shows an increasing degree of carbonization with increase in temperature. In addition, the results of analyzing solid residues at different temperatures as described earlier using FTIR are shown in Fig. 3. The absorption signal for the residual functional group appeared to decrease because of the carbonization of PEEK occurred at high temperature, with its completion at 900°C. Besides the pyrolysis of solid residue at 650°C there exists a new absorption peak in the frequency range 1720–1700 cm⁻¹. This absorption peak may be a fluorenone type structure reported by Cole et al. [7]. The mechanism of fluorenone formation was owing to the cyclization of adjacent diradicals in the ketone group as shown below:



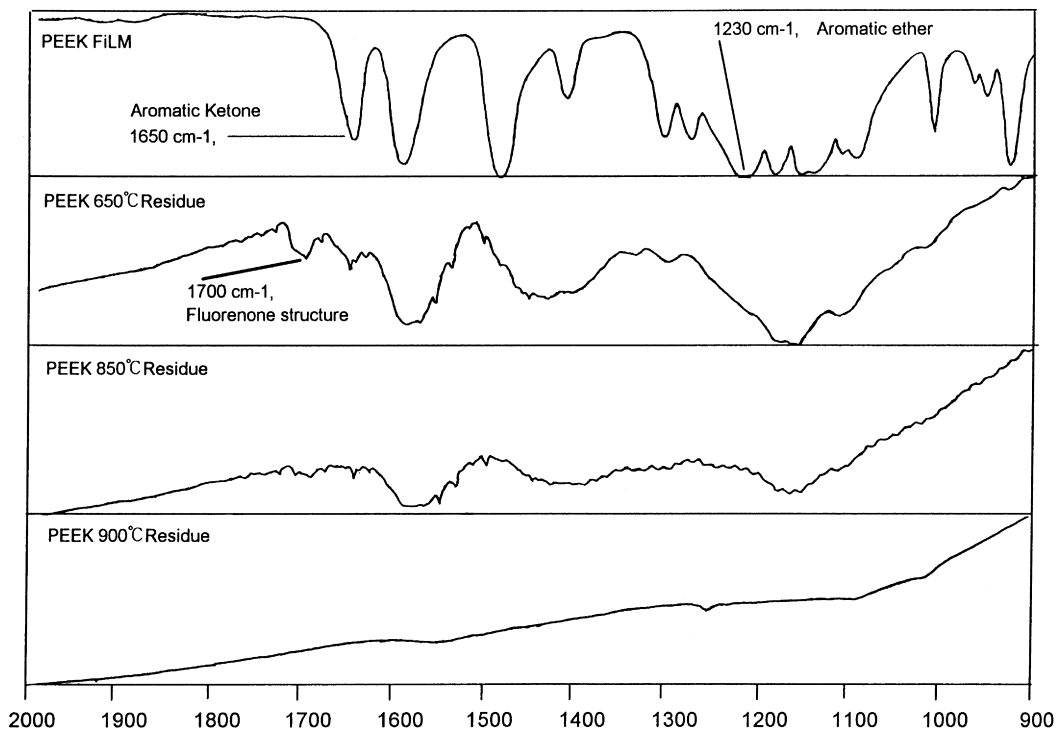


Fig. 3. FTIR spectra of solid residue from PEEK pyrolysis in He.

The main pyrolysates of PEEK in the second-stage pyrolysis region was CO_2 . Owing to the thermal stability of the fluorenone type structure being better than that of the ether group or the ketone group, we can conclude that the main pyrolysis reaction in the second-stage pyrolysis of PEEK was caused by the decomposition of this structure, which can be confirmed from the FTIR pyrogram of the solid residue at 800°C without the absorption peak at $1720\text{--}1700\text{ cm}^{-1}$ as shown in Fig. 3.

3.2. Kinetic model and parameters analysis of pyrolysis

The weight loss curve of pyrolyzed PEEK in ambient helium at a heating rate of $10^\circ\text{C}/\text{min}$ from room temperature to 900°C is shown in Fig. 1(a). This figure shows the temperature of pyrolyzed PEEK with 5% conversion to be 568°C ($T_{5\%}$). Also, the maximum pyrolysis temperatures and rates in the two pyrolysis reaction regions can be obtained, which were 575°C ($T_{\text{max}1}$) and

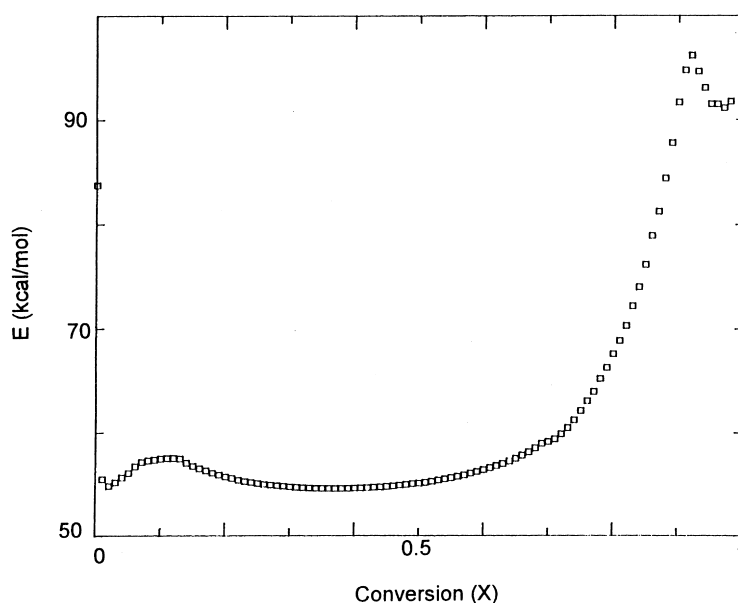


Fig. 4. Change of activation energy in PEEK pyrolysis in He.

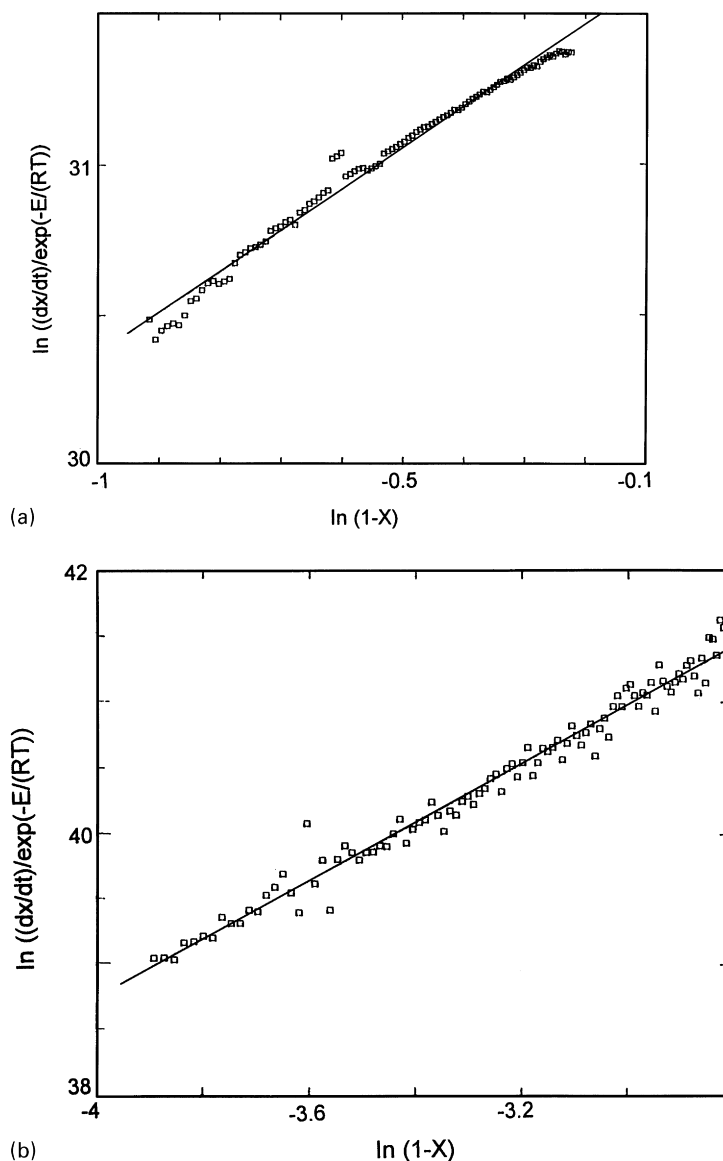


Fig. 5. Kinetic parameters in the first-stage pyrolysis of PEEK in He at 10°C/min. (b) Kinetic parameters in the second-stage pyrolysis of PEEK in He at 10°C/min.

1.05 wt%^o ($\gamma_{\max 1}$) for the first-stage pyrolysis, and 746°C ($T_{\max 2}$) and 0.08 wt%^o ($\gamma_{\max 2}$) for the second-stage pyrolysis, respectively. The solid residual weight of PEEK reached 45% when the temperature was increased to 900°C, and it became a high flame-retardant material because of its high carbonization structure. From the analytical result, the pyrolysis reaction mechanism seems to be considerably complex.

In this article, the Ozawa (1965) method [15] was used to calculate the activation energy of PEEK at different pyrolysis conversions:

$$E_a = [R \log(\beta_1/\beta_2)] / \{0.457[(1/T_1) - (1/T_2)]\} \quad (1)$$

where β is the heating rate (°C/min); T the pyrolysis temperature (K); and subscripts 1 and 2 represent different heating rates or temperatures.

The activation energy values under different conversions were calculated with heating rates of 5, 10, and 15°C/min respectively, and the conversion X can be expressed as follows:

$$X = (W_0 - W) / (W_0 - W_f)$$

where W_0 is the initial sample weight (g); W the residual weight (g) at X conversion; and W_f the final residual weight (g) at 900°C.

The calculated results are shown in Fig. 4, and two steady pyrolysis regions were observed in the conversion range of $X < 0.7$ and $X = 0.9-1.0$. In this study, the pyrolysis reaction kinetic parameters of PEEK were determined by using the activation energy values in two steady regions as described above, which can simplify the pyrolysis reaction model.

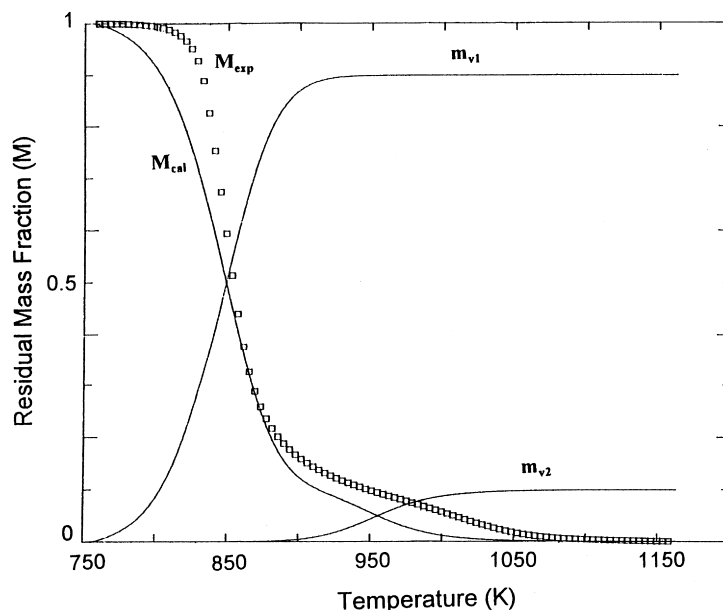


Fig. 6. Theoretical residual fractions (M_{cal} , M_{V1} , M_{V2}) and experimental value (M_{exp}) of PEEK pyrolysis in He at 10°C/min.

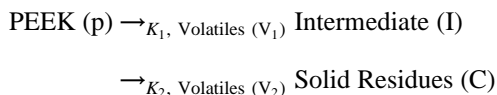
The arithmetic average activation energy values of these two steady pyrolysis regions were used, which were 55 kcal/mol at $X = 0.2-0.6$ and 92 kcal/mol at $X = 0.9-0.98$. These values matched well with previous reports [1–3]. However, these reports only focused on the lower temperature region corresponding to the first reaction region of this study, and the activation energy for the second reaction region was not mentioned.

Since $RT/E_i \ll 1$ and meets the criteria of Ozawa's method, the arithmetic average activation energy in two steady pyrolysis regions, obtained from Eq. (1), was substituted into the following rearranged equation:

$$\ln[(\partial X/\partial t)/\exp(-E_i/RT)] = \ln A + n \ln(1 - X) \quad (2)$$

where E_i is the average activation energy (kcal/mol), A the pre-exponential factor (min^{-1}), n the reaction order, T the reaction temperature (K), and X the conversion ratio.

A straight line with slope n and intercept A was obtained by plotting $\ln[(\partial X/\partial t)/\exp(-E/RT)]$ versus $\ln(1 - X)$ as shown in Fig. 5(a) and (b). Thus the reaction orders (n), pre-exponential factors (A) and arithmetic average activation energy were obtained. The n were 1.36 and 2.24 for pyrolysis reaction 1 and 2, respectively. The A were 6.02×10^{14} and $5.23 \times 10^{20} \text{ min}^{-1}$ for reactions 1 and 2, respectively. Therefore, a simplified two reaction model is proposed to present the pyrolysis of PEEK as follows:



where K_1 and K_2 are the rate constants of pyrolysis reactions 1 and 2, respectively; V_1 and V_2 are the pyrolysates of pyrolysis reactions 1 and 2, respectively.

By analyzing the pyrolysis reaction mechanism, volatile

(V_1) represents the pyrolysates listed in Table 1; intermediate (I) represents partially carbonized structure and fluorenone produced by the chain transfer from the first reaction and the cyclization of diradical respectively; and volatile (V_2) represents the CO_2 evolved mainly from the fluorenone type structure, accompanied by evolving from the *p*-benzoquinone and the large molecule of unstable carbonized structure. Simultaneously, the maximum pyrolysis temperature for the second-stage pyrolysis region in DTG profile (Fig. 1(a)) and TIC profile (Fig. 1(b)) showed slight difference. This may be explained by the fact that most of the large pyrolysates could not be detected by the TG/MS system, so the weight loss of most pyrolysates in the second-stage pyrolysis region was detected by DTG of TGA only, and not observed by TIC of the TG/MS system.

To verify the proposed model, a comparison of the computed values of the residual weight fraction by the proposed model with the experimental data need to be made. The computed values were obtained by substituting the kinetic parameters to the following equation [16,17]:

$$\begin{aligned} \frac{m_{V_i}}{F_i} &= 1 - \left[1 - (1 - n_i) \frac{A_i RT^2}{\beta E_i} \right. \\ &\quad \left. \times \exp\left(-\frac{E_i}{RT}\right) \sum (E_i, T) \right]^{(1/(1-n_i))}, \quad (n_i \neq 1) \quad (3) \end{aligned}$$

where

$$\begin{aligned} \sum (E_i, T) &= \sum_{j=0}^{\infty} \left[\left(-\frac{RT}{E_i}\right)^j \prod_{k=0}^j (k+1) \right] \\ &= 1 - 2\left(\frac{RT}{E_i}\right) + 6\left(\frac{RT}{E_i}\right)^2 - 24\left(\frac{RT}{E_i}\right)^3 + \dots \end{aligned}$$

in which F_i is the weight factor taking into account the decrease of the residual mass fraction contributed by the i pyrolysis reaction region; m_{V1} and m_{V2} are the residual mass fractions of volatiles 1 (V_1) and 2 (V_2), respectively.

Weight factors were determined from the TGA pyrogram of PEEK in ambient helium at a heating rate of 10°C/min, and they were $F_1 = 0.9$ and $F_2 = 0.1$. After substituting the weight factors into Eq. (3), theoretical values of residual mass fractions were computed as shown in Fig. 6. Therefore, the theoretical curve of M_{cal} was obtained by the following formula: $M_{\text{cal}} = 1 - (m_{V1} - m_{V2})$. In addition, the data presented in Fig. 1 have been normalized and plotted with pyrolysis temperature (K) again. The experimental curve ($M_{\text{exp}} = 1 - X$) was obtained as shown in Fig. 6, providing good agreement with the computed results of M_{cal} for the proposed model. However, the calculated curve shifted to lower temperature in comparison with experimental data, showing the actual thermal stability of PEEK to be higher than predicted, which may be explained by the formation of fluorenone structure at the initial pyrolysis of PEEK. The degree of carbonized solid residue increased gradually and carbonization became the dominant mechanism when pyrolysis proceeded from the first-stage pyrolysis region to the second-stage pyrolysis region. But this did not consider the kinetic model, so the theoretical pyrolysis curve shifted to lower temperature in comparison with the experimental curve, which indicated that the prediction of thermal stability for this material was lower than the actual one.

4. Conclusions

A new analytical technique performed satisfactorily by coupling Py-GC/MSs good separating ability of pyrolysates in analysis and TG/MSs ability for real time monitoring of pyrolysates. More details about the pyrolysis mechanism could be gained by decreasing the complexity of the TG/MS diagram using selective ion to analyze real time curves of major pyrolysates. It was confirmed that the combination of Py-GC/MS and TG/MS analytical techniques could provide additional insight into the pyrolysis mechanism of polymeric materials.

The experimental results indicated that the pyrolysis of PEEK in helium atmosphere covering a temperature range from room temperature to 900°C, could be attributed to the two-stage stable pyrolysis regions. At the first-stage stable

pyrolysis region, main chain random scission was the primary pyrolysis mechanism which included the cleavage of ether group to yield phenol as the major pyrolysis product at lower temperature and the decomposition of ketone group to yield CO₂ as the major pyrolysis product at higher temperature. Also, the main chain random scission was accompanied by chain transfer which included: the formation of carbonized solid residue and cyclization of diradical from adjacent benzene radicals in the ketone group to yield the fluorenone type structure. At the second-stage pyrolysis region, the primary pyrolysis mechanism was the cleavage of the fluorenone type structure to yield CO₂.

The pyrolysis mechanism and chemical kinetic model of polymeric material was presented simultaneously for the first time. The detailed explanation for the formation of pyrolysates and reaction model was proposed. Based on the hypothesis and calculation of the proposed model, the arithmetic average activation energy, reaction order and pre-exponential factor in different pyrolysis regions can be obtained.

Acknowledgements

We thank the National Science Council of the Republic of China for financial support throughout this work.

References

- [1] Day M, Cooney JD, Wiles DM. *Polym Eng Sci* 1989;29:19.
- [2] Day M, Cooney JD, Wiles DM. *J Appl Polym Sci* 1989;38:323.
- [3] Day M, Cooney JD, Wiles DM. *Thermochim Acta* 1989;147:189.
- [4] Kenny JM, Torre L, Nicolais L. *Thermochim Acta* 1993;227:97.
- [5] Salin JM, Seferis JC. *J Appl Polym Sci* 1993;47:847.
- [6] Hay JN, Kemmish DJ. *Polymer* 1987;28:2047.
- [7] Cole KC, Casella IG. *Polymer* 1993;34:740.
- [8] Day M, Cooney JD, Wiles DM. *J Anal Appl Pyrolysis* 1990;18:163.
- [9] Sato H, Kikuchi T, Koide N, Furuya K. *J Anal Appl Pyrolysis* 1996;37:173.
- [10] Matushek G. *Thermochimica Acta* 1995;263:59.
- [11] Moulinie P, Paroli RM, Wang ZY, Delgado AH, Guen AL, Gi Y, Gao JP. *Polym Testing* 1996;15:75.
- [12] Nam JD, Seferis JC. *J Polym Sci Part B: Polym Phys* 1992;30:455.
- [13] Perng LH, Tsai CJ, Ling YC. To be published.
- [14] Tsai CJ, Perng LH, Ling YC. *Mass Spectrometry* 1997;11:1987.
- [15] Ozawa T. *Bull Chem Soc Jpn* 1965;38:1881.
- [16] Chang CY, Wu CH, Hwang JY, Lin JP, Yang WF, Shin SM, Chen LW, Chang FW. *J Environ Eng* 1996;122:1.
- [17] Lin JP, Chang CY, Wu CH. *J Chem Tech Biotechnol* 1996;66:1.